REVIEW ARTICLE

WILEY

Spectrum of clinical applications of interlead ECG heterogeneity assessment: From myocardial ischemia detection to sudden cardiac death risk stratification

Richard L. Verrier PhD [ID] | Bruce D. Nearing PhD | Andre D'Avila MD, PhD

Division of Cardiovascular Medicine, Department of Medicine, Beth Israel Deaconess Medical Center, Harvard Medical School, Boston, Massachusetts, USA

Correspondence
Richard L. Verrier, Division of Cardiovascular Medicine, Department of Medicine, Beth Israel Deaconess Medical Center, Harvard Medical School, 99 Brookline Avenue, RN-301, Boston MA 02215-3908, USA.
Email: rverrier@bidmc.harvard.edu

Abstract

Heterogeneity in depolarization and repolarization among regions of cardiac cells has long been recognized as a major factor in cardiac arrhythmogenesis. This fundamental principle has motivated development of noninvasive techniques for quantification of heterogeneity using the surface electrocardiogram (ECG). The initial approaches focused on interval analysis such as interlead QT dispersion and T_{peak}–T_{end} difference. However, because of inherent difficulties in measuring the termination point of the T wave and commonly encountered irregularities in the apex of the T wave, additional techniques have been pursued. The newer methods incorporate assessment of the entire morphology of the T wave and in some cases of the R wave as well. This goal has been accomplished using a number of promising vectorial approaches with the resting 12-lead ECG. An important limitation of vectorcardiographic analyses is that they require exquisite stability of the recordings and are not inherently suitable for use in exercise tolerance testing (ETT) and/or ambulatory ECG monitoring for provocative stress testing or evaluation of the influence of daily activities on cardiac electrical instability. The objectives of the present review are to describe a technique that has been under clinical evaluation for nearly a decade, termed "interlead ECG heterogeneity." Preclinical testing data will be briefly reviewed. We will discuss the main clinical findings with regard to sudden cardiac death risk stratification, heart failure evaluation, and myocardial ischemia detection using standard recording platforms including resting 12-lead ECG, ambulatory ECG monitoring, ETT, and pharmacologic stress testing in conjunction with single-photon emission computed tomography myocardial perfusion imaging.

KEYWORDS
ECG heterogeneity, heart failure, myocardial ischemia, sudden cardiac death risk stratification, T-wave alternans, ventricular arrhythmias

1 | ECG HETEROGENEITY CONCEPT: DEFINITION AND RATIONALE FOR USE IN ARRHYTHMIA RISK STRATIFICATION

Electrocardiographic (ECG) heterogeneity is defined as nonuniformity in depolarization and repolarization, which lead to heterogeneity of R-wave and T-wave morphology (Antzelevitch, 2007; Fuller et al., 2000; Prenner et al., 2016; Weiss et al., 2005). The terms *heterogeneity* and *dispersion* have been used synonymously in the experimental and clinical literature (Surawicz, 1996); in the current review, the former designation will be employed. As regions of the normal ventricular myocardium do not activate or inactivate simultaneously, some degree of ECG heterogeneity is necessary for normal cardiac function and is responsible for the generation of the QRST complex. The adaptive advantage of heterogeneous sequential activation of the ventricles from apex to base is to achieve efficient pumping action of the heart. The depolarization waveform orchestrates the inotropic action of ionized calcium to optimize the contractile function of the myocytes.

ECG heterogeneity in the diseased myocardium is fundamentally linked to development of unidirectional block and reentry, precursors of ventricular arrhythmias. This principle was highlighted in classic studies by Han and Moe (1964), who performed electrical stimulation to demonstrate the connection between nonuniformities in tissue refractoriness and vulnerability to ventricular fibrillation (VF). ECG heterogeneity is associated with arrhythmias in a variety of conditions including myocardial ischemia, infarction, sympathetic stimulation, and several channelopathies, notably the long QT and Brugada syndromes (Antzelevitch, 2007). Heterogeneity can be categorized as either temporal, reflecting variations over time, or spatial, among different regions of the heart. In general, under disease conditions, multiple types of heterogeneity coexist and are termed spatiotemporal. Collectively, these electrophysiological relationships provide sound underpinnings for the assessment of ECG heterogeneity for determining risk for ventricular arrhythmias and sudden cardiac death (SCD).

2 | CONTEMPORARY CLINICAL APPROACHES

In the 1990s, Higham and Campbell (1994) engendered considerable interest with the introduction of QT interval dispersion on standard 12-lead ECGs as a marker of arrhythmia risk. The method and concept were relatively straightforward, involving simply searching for the largest differences in the QT interval across the entire lead set. This approach prompted a sizeable literature of >1000 publications. However, it has fallen into disfavor because of significant conceptual and methodological limitations (Rautaharju, 2002). These are mainly related to inaccuracies in determining the end of the T wave (Prenner et al., 2016) and uncertainty about whether QT interval differences across the 12-lead set adequately represent the electrophysiological property of heterogeneity (Malik et al., 2000).

Numerous techniques have since been developed, particularly analysis of the T_{peak}–T_{end} interval, which has been employed as an alternative interval-based measure for heterogeneity of repolarization (Antzelevitch, 2007). However, this technique has achieved only mixed results in predicting SCD (Panikkath et al., 2011; Porthan et al., 2013). The inconsistent results have been attributed to difficulties similar to those with QT dispersion, specifically irregularities in the apex and termination of the T wave.

Alternative approaches to ECG heterogeneity analysis have involved assessing the entire morphology of the T wave (Malik et al., 2000; Nearing & Verrier, 2003, 2015; Porthan et al., 2009; Okin et al., 2000; Zabel et al., 2000). A number of vectorial approaches have been developed including Principal Component Analysis Ratio, T-wave morphology dispersion, Total Cosine R-to-T, and T-wave residuum (Porthan et al., 2009; Verrier & Huikuri, 2017). Overall, it appears that the use of quantitative vector loop analyses to characterize heterogeneity of depolarization and repolarization morphology in resting 12-lead ECGs adds to the predictive armamentarium for identifying risk for SCD. In the largest vectorcardiographic study, "Atherosclerosis Risk in Communities" (ARIC), Waks et al. (2016) determined that global electrical heterogeneity is independently associated with SCD in the general population. These innovative approaches clearly characterize ECG heterogeneity in a manner that goes well beyond the QT interval. However, most vectorcardiographic methods do not provide information regarding the independent contributions of depolarization and repolarization heterogeneity to arrhythmia risk.

An important limitation of vectorcardiographic analyses is that they require exquisite stability of the recordings and are not inherently suitable for use in exercise tolerance testing (ETT) and/or ambulatory ECG monitoring. As a consequence, these methods do not incorporate the physiologic and pharmacologic challenges that are employed in routine clinical evaluation or the stresses of daily activity, which serve to disclose latent susceptibility to ventricular arrhythmias and underlying coronary artery disease.

3 | MAIN GOALS OF THE REVIEW

The objectives are multifold: (1) To describe the second central moment technique for analysis of interlead R-wave and T-wave heterogeneity; (2) To review the experimental studies and electrophysiological evidence underlying its capacity to predict arrhythmia; (3) To discuss the main clinical applications of the method with reference to its use during standard clinical evaluation including the resting 12-lead ECG, ambulatory ECG monitoring, ETT, and pharmacologic stress testing in conjunction with single-photon emission computed tomography myocardial perfusion imaging (SPECT MPI).

3.1 | Tracking interlead heterogeneity of R- and T-wave morphology by second central moment analysis

A nonvector ECG analysis approach has been developed that is based on principles from Newtonian mechanics, termed "second

FIGURE 1 Flowchart of signal processing and computing of the second central moment calculation of R-wave heterogeneity (RWH) and T-wave heterogeneity (TWH) in a representative patient with cardiomyopathy with ventricular tachycardia (VT) (left panel), who exhibited greater splay (heterogeneity) than did the patient with cardiomyopathy without VT (right panel). Electrocardiograms were simultaneously obtained from precordial leads V_4, V_5, and V_6. Reprinted with permission from Verrier and Huikuri (2017)
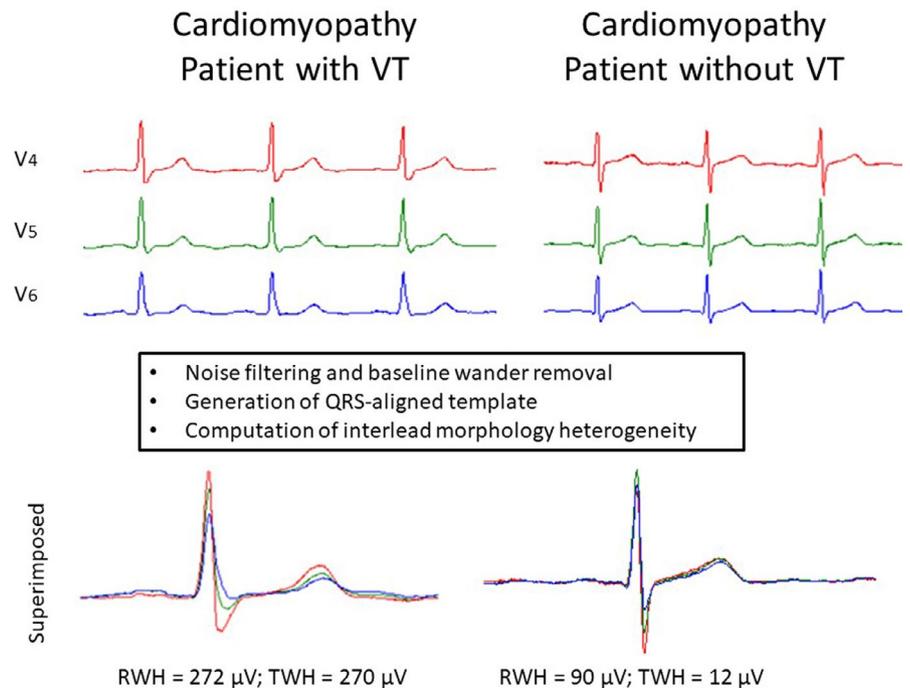

FIGURE 2 Crescendo in depolarization and repolarization heterogeneity [R-wave heterogeneity (RWH) (□), T-wave heterogeneity (TWH) (■)] (lower panel), culminating in T-wave alternans (TWA) and ventricular tachycardia (VT) (upper panel) in lead V_5 in a patient enrolled in the Prospective Randomized Evaluation of Cardiac Ectopy with Dobutamine or Nesiritide Therapy (PRECEDENT) trial. Reprinted with permission from Nearing et al. (2012)
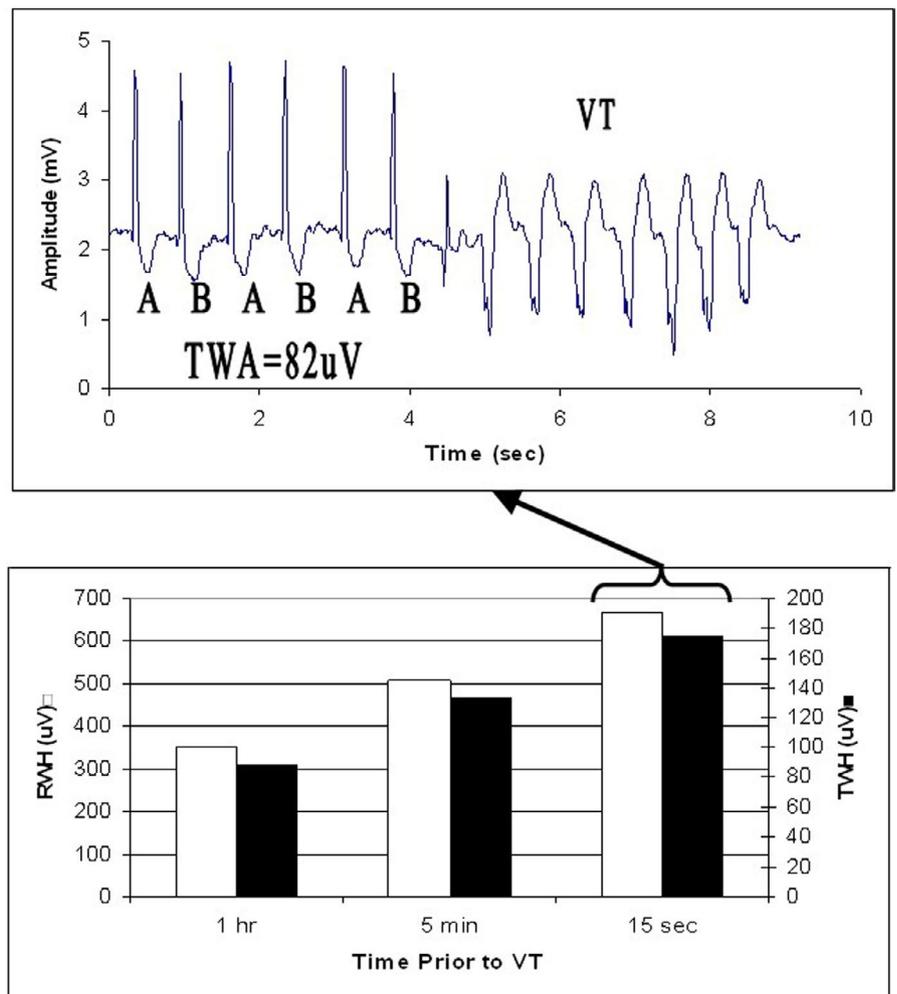
central moment" (Nearing & Verrier, 2003; 2015). The method is depicted in ECGs obtained from patients with cardiomyopathy with and without ventricular tachycardia (VT) (Figure 1) (Verrier & Huikuri, 2017). Essentially, signal processing software generates separate mean morphologies (the "first moment") for the QRS intervals and T waves. Then, the splay or heterogeneity in morphology

about this mean axis (the "second moment") is calculated by taking the square root of the variance about the mean morphology. Thus, the method is quantitative and incorporates the morphology of the entire waveform, as opposed to calculating solely the duration of the intervals. QRS-aligned templates are developed to enable visualization of the heterogeneity or splay in morphology for review together with a quantitative output in microvolts.

Second central moment analysis allows assessment of both depolarization and repolarization morphology heterogeneity using a single tool and therefore affords an important insight into their relative contributions to arrhythmia susceptibility. In healed postinfarct myocardium, abnormal conduction occurs through an infarct border zone resulting from altered connectivity of surviving myocytes, which are encased in fibrous tissue strands, and gap junctional components of intercalated discs during remodeling (Wit & Janse, 1992). Abnormal conduction through diseased myocardium, whether as a result of gross structural remodeling of scarred myocardium or subcellular ionic or gap junctional remodeling, may manifest as interlead splay of ECG waveforms. Ultimately, ventricular arrhythmias develop from a dynamic interaction of both depolarization and repolarization heterogeneity.

A distinct feature of R-wave and T-wave heterogeneity (RWH and TWH) is that this analytical approach provides temporospatial information as it involves signals from three to five leads compared with a single lead in the case of QT dispersion or QRS complex duration. The central tenet tested is that multilead ECG morphology analysis provides an improved assessment of the underlying action potential patterns and their coupling to contractile synergy via the biophysical factors at the root of excitation–contraction coupling.

3.2 | Experimental studies

Interlead heterogeneity of morphology has been investigated extensively in large animal models since its introduction in 2003 (Bonatti et al., 2014; Fuller et al., 2016; Justo et al., 2016; Nearing & Verrier, 2003; Verrier et al., 2013; Zhao et al., 2006). During acute myocardial ischemia, TWH was shown to exhibit a crescendo in amplitude, heralding the development of VF. An orderly progression in TWH magnitude preceded high levels of T-wave alternans (TWA) followed by discordant TWA and culminated in VT/VF (Nearing & Verrier, 2003). These observations concur with the well-established integral relationship between TWH and alternation of the T wave (Chauhan et al., 2006; Nearing & Verrier, 2003; Verrier et al., 2009). It is noteworthy that in patients with decompensated heart failure, RWH and TWH similarly exhibited a crescendo before TWA and VT (Figure 2) (Nearing et al., 2012). Accordingly, they could constitute a warning sign for impending TWA and malignant arrhythmia. High levels of TWH were also observed in experimental studies in response to profibrillatory conditions such as partial coronary artery stenosis (Bonatti et al., 2014; Verrier et al., 2013) with and without adrenergic stimulation (Fuller et al., 2016; Justo et al., 2016) and excess intracoronary calcium (Zhao et al., 2006).

4 | CLINICAL APPLICATIONS OF INTERLEAD R-WAVE AND T-WAVE HETEROGENEITY BY SECOND CENTRAL MOMENT ANALYSIS

The main conditions in which this technique has been investigated include the following: (1) SCD risk stratification using resting 12-lead ECGs and electrophysiology laboratory equipment; (2) arrhythmogenesis in patients with heart failure monitored on 12-lead or ambulatory ECGs; and (3) detection of clinically significant coronary artery disease during ETT or pharmacologic stress testing. The clinical applications of ECG heterogeneity tested to date are summarized in Table 1.

4.1 | Cardiac mortality and SCD risk assessment from resting 12-lead ECGs

The suitability of second central moment analysis of interlead RWH, J-wave heterogeneity (JWH), and TWH to assess risk for SCD was studied in the sizable 5600-subject Health Survey 2000 (Kenttä et al., 2016). The 12-lead resting ECGs were obtained using a standard clinical acquisition system (MAC5000 electrograph with QT guard, GE Healthcare, Milwaukee WI, USA). Representative median beats for each of the 12 leads were derived from the 10-second ECG recordings. Fully automated second central moment analysis was performed on the median beats to quantify spatial RWH, JWH, and TWH. The system has high-throughput efficiency, evidenced by the fact that the entire database of 5600 patients was analyzed within 15 min, at a rate of <1 s per subject. The adjusted odds for SCD and cardiac death risk were 1.7–3.2 and 2.1–3.5, respectively (Table 1). The QRS-aligned TWH template for a subject who survived across the 8-year follow-up period was compared with that of a subject who succumbed to SCD (Figure 3, upper panel). In the latter case, the splay in the three components of the waveforms is apparent. The Kaplan–Meier mortality curves are provided (Figure 3, lower panels). When RWH, JWH, and TWH were all abnormal, the adjusted relative risk for SCD was 3.2 (95% CI 1.4–7.1; $p = .009$) (Table 1). The value of combining RWH, JWH, and TWH in screening the general population is evident in Table 2, as the adjusted odds ratio of 3.2 is more than double that obtained from any independent vectorcardiographic parameter. Thus, the measurement of interlead ECG heterogeneity provides an ultra-rapid means for analysis of ECGs in large volumes of data and holds promise for screening general populations.

4.2 | Electrophysiologic study laboratory 12-lead ECG predicts VT/VF/ICD discharge and arrhythmic death in cardiomyopathy patients

The investigation was carried out in 120 consecutive patients with cardiomyopathy without an apparent reversible trigger for VT, recent myocardial infarction, or active ischemia, who presented for

TABLE 1 Clinical applications of ECG heterogeneity

	Cohort	Publication	Adjusted Odds Ratio	AUC
SCD and cardiac death risk assessment in resting 12-lead ECG	Health Survey 2000; general population, n = 5618	Kenttä et al., 2016	1.7–3.2 for SCD; 2.1–3.5 for cardiac death	NR
	Cardiomyopathy during EP study, single center, n = 120	Tan et al., 2017	NR	0.71 (3-dimensional)
	Emergency department, single center, 90-day mortality, n = 100	Monteiro et al., 2021	Women: 121.4; Men: 2.9	0.933 for women 0.573 for men
Arrhythmia risk assessment in heart failure patients with reduced LVEF	Hospitalized patients with decompensated heart failure in PRECEDENT trial	Nearing et al., 2012	NR	NR
	CRT patients, single center, n = 155	Bortolotto et al., 2020	19.1–43.0 for RWH, 9.5–24.0 for TWH in predicting super-response to CRT in patients with non-LBBB	0.891 for RWH in predicting super-response to CRT in patients with non-LBBB
	ANTHEM-HF Pilot study, n = 25	Nearing et al., 2021	NR	NR
Detection of clinically significant coronary stenosis	Referred for ETT or pharmacological stress testing with dipyridamole, single center, n = 137	Silva et al., 2020	ETT = 5.26; dipyridamole stress = 30.22	ETT = 0.737; dipyridamole stress = 0.818
	Referred for pharmacological stress testing with regadenoson, single center, n = 103	Araujo Silva et al., 2020	Men = 7.3; women = 4.5	Men = 0.79; women = 0.71

Abbreviations: CRT, cardiac resynchronization; EP, electrophysiologic; ETT, exercise tolerance testing; non-LBBB, non-left bundle branch block; NR, not reported; RWH, R-wave heterogeneity; SCD, sudden cardiac death; TWH, T-wave heterogeneity.
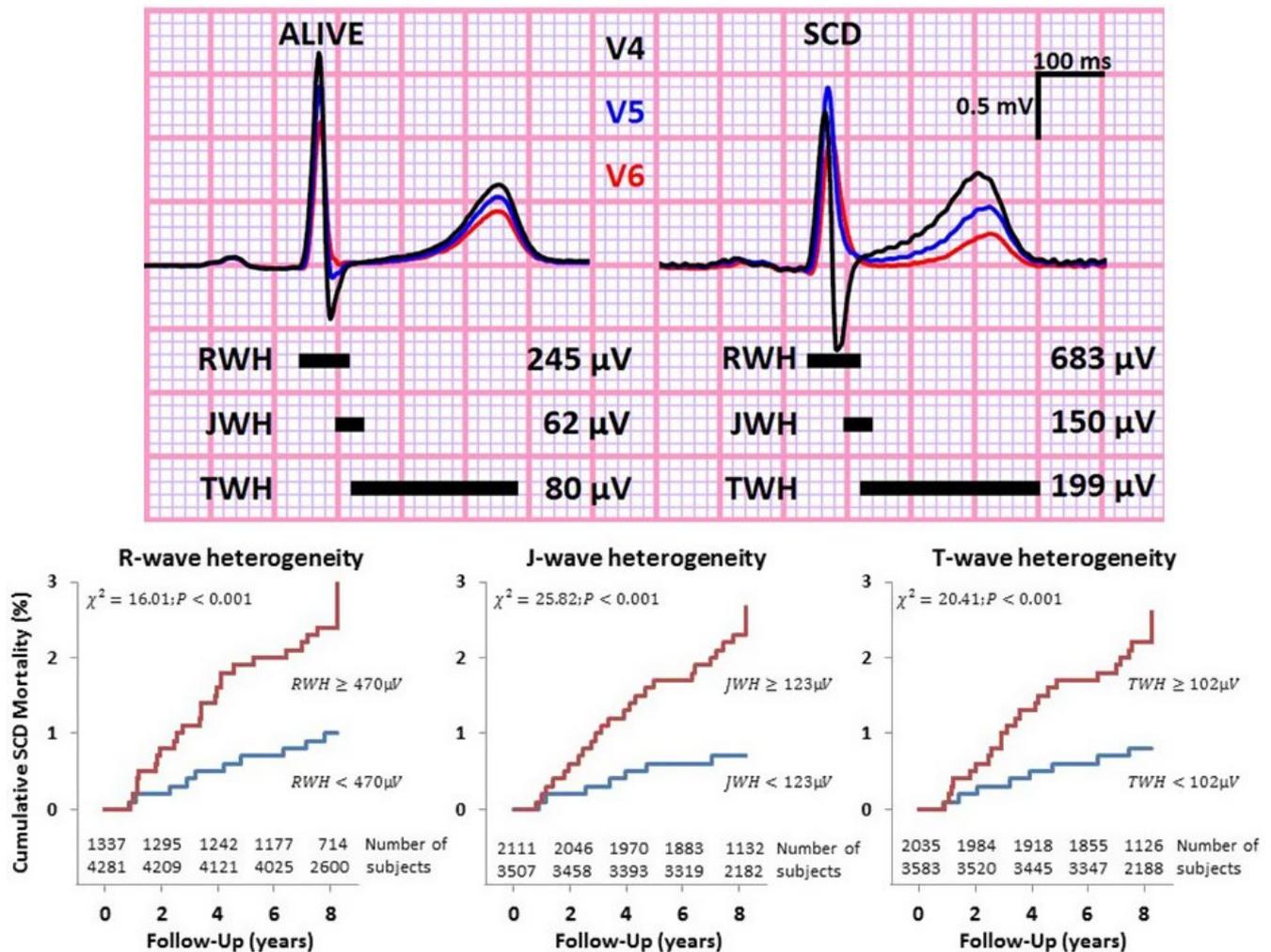
FIGURE 3 Upper panel: Superimposed left precordial lead electrocardiograms (leads V_4–V_6) recorded in a survivor (left) and in a subject who suffered sudden cardiac death (SCD) (right) during the follow-up period from Health Survey 2000 illustrate R-wave heterogeneity (RWH), J-wave heterogeneity (JWH), and T-wave heterogeneity (TWH). Black horizontal bars indicate the periods when RWH, JWH, and TWH were measured. Lower panel: Kaplan–Meier curves of RWH, JWH, and TWH for SCD with numbers of subjects. Reprinted with permission from Kenttä et al. (2016)

electrophysiologic study, implantable cardioverter-defibrillator (ICD) placement, or generator change at our institution from 2008 to 2011 (Tan et al., 2017). The primary outcome was sustained VT/VF or appropriate ICD therapies. The secondary outcome was arrhythmic death or resuscitated cardiac arrest. The cut-points for abnormal RWH (>160 μV) and TWH (>80 μV) identified 67% of primary outcome cases and 85% of secondary outcome cases. Patients with cardiomyopathy who met the primary outcome ($n = 42$) had significantly higher TWH than those who did not ($n = 28$) (95 ± 11 vs. 44 ± 9 μV, $p < .002$). Similarly, cardiomyopathy patients who met secondary outcome ($n = 13$) had VT/VF during follow-up and also had significantly higher TWH than survivors ($n = 57$) (105 ± 24 vs. 67 ± 8 μV, $p < .002$). Kaplan–Meier analysis disclosed significant differences in arrhythmia-free survival ($p = .012$) and total survival ($p = 0.011$) among cardiomyopathy patients with ($n = 37$) versus those without ($n = 33$) elevated RWH and/or TWH independent of age, sex, and left ventricular

ejection fraction (LVEF). The Kaplan–Meier mortality curves are provided (Figure 4). These findings demonstrated that interlead RWH and TWH in resting 12-lead ECGs predict sustained ventricular arrhythmia, appropriate ICD therapies, and arrhythmic death or cardiac arrest in cardiomyopathy patients independent of LVEF and other standard variables.

4.3 | TWH in 12-lead ECGs for prediction of 90-day cardiac mortality following emergency department admission for acute coronary syndrome

Coronary heart disease claimed >840,000 lives in 2016 in the United States (Virani et al., 2020). Solomon and colleagues (2005) underscored the pressing need for improved monitoring of SCD risk. In the Valsartan in Acute Myocardial Infarction Trial (VALIANT), which enrolled >14,000 patients, they observed that SCD risk was highest

TABLE 2 Contemporary analytical approaches to sudden cardiac death risk stratification in Health Survey 2000

Electrocardiographic marker	Multivariable adjusted odds ratio for sudden cardiac death (95% CI)	Significance (*p* values)
Interval markers in single leads		
QT_{NC}	1.2 (1.01–1.5)	.044
QT_F	1.2 (0.996–1.5)	.054
$T_{peak}–T_{end}$ in lead V_5	0.9 (0.8–1.2)	.620
Vectorcardiographic markers		
Principal component analysis ratio	1.1 (0.9–1.4)	.367
T-wave morphology dispersion	1.4 (1.1–1.7)	.001
Total cosine R-to-T	1.3 (1.1–1.6)	.013
T-wave residuum	1.2 (1.0–1.5)	.050
Second central moment in multiple leads		
RWH (≥470 mV)	1.2 (0.8–2.0)	<.05
JWH (≥123 mV)	2.0 (1.2–3.3)	<.01
TWH (≥102 mV)	1.7 (1.0–2.9)	<.05
JWH + TWH	2.9 (1.5–5.7)	<.01
RWH + JWH + TWH	3.2 (1.4–7.1)	<.01

Abbreviations: CI, confidence interval; JWH, J-wave heterogeneity; QT_F, QT interval with the Frederica formula for adjustment of heart rate; QT_{NC}, QT interval with the nomogram method for adjustment of heart rate; RWH, R-wave heterogeneity; TWH, T-wave heterogeneity.

Data are from Kenttä et al. (2016) and Porthan et al. (2013). Table is reprinted with permission from Verrier and Huikuri (2017)

in the first few months after myocardial infarction among patients with or without significant heart failure.

We investigated whether repolarization heterogeneity could identify patients who are at risk for near-term cardiac mortality following discharge from the emergency department for acute coronary syndrome evaluation to rule-in or rule-out myocardial infarction (Monteiro et al., 2021). TWH_{V4-6} was significantly elevated at emergency department admission in 12-lead resting ECGs of female patients who died of cardiac causes during the following 90 days compared with female survivors (100 ± 14.9 vs. 40 ± 3.6 μV, $p < .0001$). TWH_{V4-6} yielded areas under the receiver operating characteristic (ROC) curve (AUC) of 0.933 in women ($p < .0001$) and 0.573 in men ($p = .4$) (Table 1). In women, the ROC-guided 48-μV TWH_{V4-6} cutpoint for near-term cardiac mortality generated an adjusted odds ratio of 121.4 (95% CI: 2.89–6699.84; $p = .02$) with 100% sensitivity and 82.5% specificity. In Kaplan–Meier survival analysis, $TWH_{V4-6} \geq 48$ μV predicted cardiac mortality in women during 90-day follow-up with a hazard ratio of 27.84 (95% CI: 7.29–106.36, $p < .0001$). It was concluded that elevated TWH_{V4-6} is associated with near-term cardiac mortality among women evaluated for acute coronary syndrome. The capacity to stratify arrhythmia risk in patients with healed myocardial infarction is under investigation.

4.4 | Arrhythmia risk assessment in hospitalized patients with decompensated heart failure

There is a critical need for reliable warning markers of in-hospital malignant arrhythmias. Nearing and colleagues (2012) performed a nested case–control analysis of pre-randomization ambulatory ECGs (leads V_1, V_5, and aVF) of patients ($n = 44$) enrolled in the Prospective Randomized Evaluation of Cardiac Ectopy with Dobutamine or Nesiritide Therapy (PRECEDENT) trial. RWH and TWH were determined by second central moment analysis and TWA by modified moving average analysis (Verrier et al., 2011). Of the 44 PRECEDENT patients studied, 22 had experienced epochs of VT after 120 min of stable sinus rhythm; 22 patients without VT were selected from among the trial enrollees matched for age and sex. TWA magnitude increased significantly in lead V_5 at 15–30 min before VT and remained high until the arrhythmia ensued. RWH and TWH were elevated from 30 to 45 min before VT, preceding the crescendo in TWA by 15 min. Matched patients without VT did not exhibit elevated RWH or TWH during the 24-h period. Based on these observations, it was concluded that depolarization and repolarization heterogeneity have the capacity to detect crescendos in cardiac electrical instability that could forewarn of impending TWA and nonsustained VT (NSVT) (Figure 2).

4.5 | ECG Heterogeneity for predicting mechanical response and mortality in CRT patients

Cardiac resynchronization therapy (CRT) is an important treatment for patients with advanced heart failure and left ventricular conduction delay with and without left bundle branch block (LBBB). CRT has been proven to relieve symptoms, increase functional capacity, and prolong life in many cases, but the response rates have ranged from 32% to 91% depending on the criteria employed
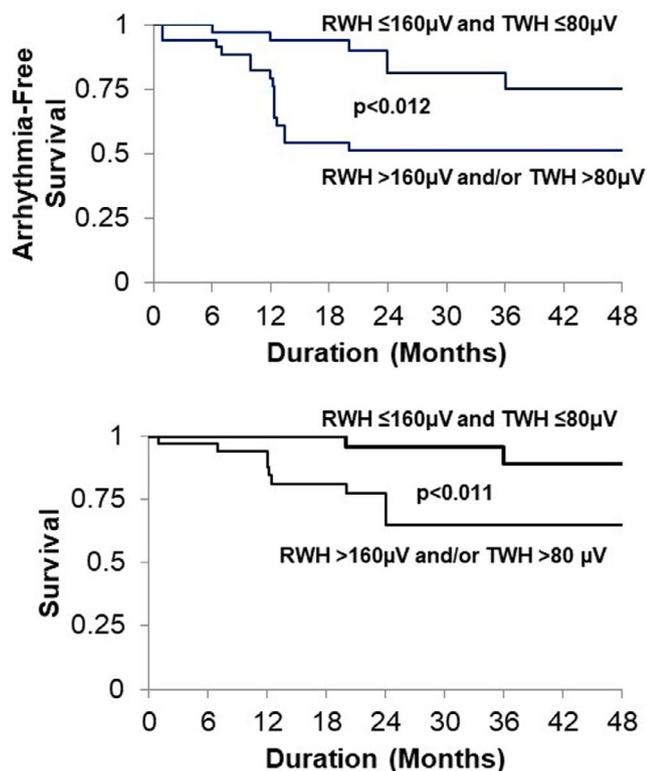
FIGURE 4 Arrhythmia-free survival (upper panel) and total survival (lower panel) in all cardiomyopathy (CM) patients (*n* = 70) according to Kaplan–Meier plots. CM patients with arrhythmic events (*n* = 42) exhibited elevated interlead R-wave morphology heterogeneity (RWH) (>160 μV) and/or T-wave morphology heterogeneity (TWH) (>80 μV) compared with those without events (*n* = 28, *p* = .012). CM patients who died (*N* = 6) or were resuscitated (*N* = 7) had elevated RWH (>160 μV) and/or TWH (>80 μV) compared with survivors (*n* = 57, *p* = .011). Reprinted with permission from Tan et al. (2017)

(Moss et al., 2009; Tomassoni, 2016). The most commonly used ECG criterion, QRS complex duration, performs more poorly than qualitative clinical predictors of CRT response (Dupont et al., 2012; Rickard et al., 2010). Thus, more reliable quantitative predictors are needed.

Bortolotto and colleagues (2020) examined whether preimplantation interlead ECG heterogeneity might be superior to QRS complex duration in predicting mechanical super-response to CRT. Super-responder status was defined as ≥20% increase in LVEF and/ or ≥20% decrease in left ventricular end-systolic diameter (Rickard et al., 2010). Super-responders (*n* = 35, 23%) were compared with non-super-responders (*n* = 120, 77%), who did not meet these criteria. Among patients with non-left bundle branch block (non-LBBB), preimplantation RWH was significantly lower in super-responders than in non-super-responders in three of four lead sets (*p* = .001 to *p* = .038) and preimplantation TWH was significantly lower in two lead sets (both *p* = .05). The corresponding odds ratios (RWH: 19.1–43.0; *p* = .003 to *p* = .03; TWH: 9.5–24.0; *p* = .008 to *p* = .05) and AUCs (RWH: 0.810–0.891, *p* = .001; TWH: 0.759–0.810, *p* = .005) for predicting mechanical super-response to CRT (Figure 5) were

highly significant (Table 1). No differences were found in the LBBB group. Preimplantation QRS complex duration in super-responders also was not different from in non-super-responders among patients with (*p* = .856) or without (*p* = .724) LBBB; the AUCs were non-significant (both, *p* = .69). RWH$_{V1-3LILII}$ >420 mV predicted 3-year all-cause mortality in the entire cohort (*p* = .037) with a hazard ratio of 7.440 (95% confidence interval 1.015–54.527; *p* = .048); QRS complex duration >150 ms did not predict mortality (*p* = .27). These results led to the conclusion that preimplantation ECG heterogeneity is superior to QRS complex duration in predicting mechanical super-response to CRT in patients with non-LBBB. Patients with higher RWH and TWH levels are less likely to benefit from CRT than those with lower levels. The precise electrophysiological basis for the suitability of preimplantation RWH and TWH to predict super-mechanical response, especially in comparison to QRS complex duration, requires follow-up. The recent demonstration that ECG heterogeneity correlates with speckle tracking strain measures and mechanical dispersion in patients experiencing conduction abnormalities induced by transcatheter aortic valve replacement may provide some clues regarding mechanisms (Burke et al, in press).

4.6 | Detection of improvement in cardiac electrical instability in patients receiving VNS therapy

Individuals with heart failure with reduced LVEF (HFrEF) experience long-term deterioration of autonomic function and cardiac electrical stability resulting in increased mortality risk. The Autonomic Neural Regulation Therapy to Enhance Myocardial Function in Heart Failure (ANTHEM-HF) Pilot study reported improved heart rate variability (HRV), baroreceptor sensitivity as indicated by heart rate turbulence (HRT), and reduced TWA and numbers of patients with NSVT after 12 months of vagus nerve stimulation (VNS) therapy (Libbus et al., 2016). Recently, an analysis was performed to determine whether the benefits of chronic VNS persist in the long term. The effects of chronic VNS were assessed in all ANTHEM-HF patients with ambulatory ECG data at follow-up at 24 and 36 months (*n* = 25) (Nearing et al., 2021). Autonomic markers improved significantly at 24 and 36 months compared with baseline (*p* < .05) (Figure 6). Peak TWA levels remained reduced at 24 and 36 months (*p* < .0001). The decreases in RWH and TWH at 6 and 12 months persisted at 24 and 36 months (*p* < .01). Numbers of patients with NSVT decreased at 12, 24, and 36 months (*p* < .025). There were no occurrences of SCD or of VF or sustained VT on ambulatory ECG.

Notably, VNS also exerted a sustained, substantial effect across 3 years in improving LVEF, six-minute walk test, and New York Heart Association (NYHA) class (Figure 7). NYHA class was improved in 96% of subjects. The potential mechanisms for improvement in LVEF include the fact that VNS has been demonstrated experimentally to protect cardiac myocytes by decreasing oxidative stress, apoptosis, inflammatory response, and the cardiotoxic effects of excessive levels of catecholamines through muscarinic-receptor-mediated accentuated antagonism (Kolman et al., 1975; Levy & Blattberg, 1976; Li &
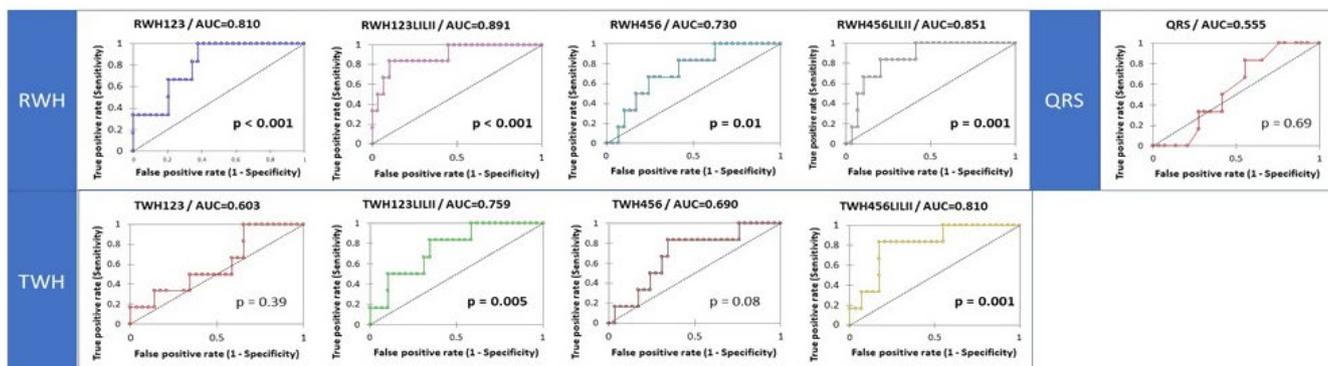
FIGURE 5 Receiver operating characteristic (ROC) curves for the capacity of R-wave heterogeneity (RWH) and QRS complex duration to predict mechanical super-response to cardiac resynchronization therapy in patients without left bundle branch block (non-LBBB). RWH in all lead sets showed significance in non-LBBB patients. The p value is based on the difference between the areas under the curve (AUCs) and an AUC of 0.5 (random). Reprinted with permission from Bortolotto et al. (2020)
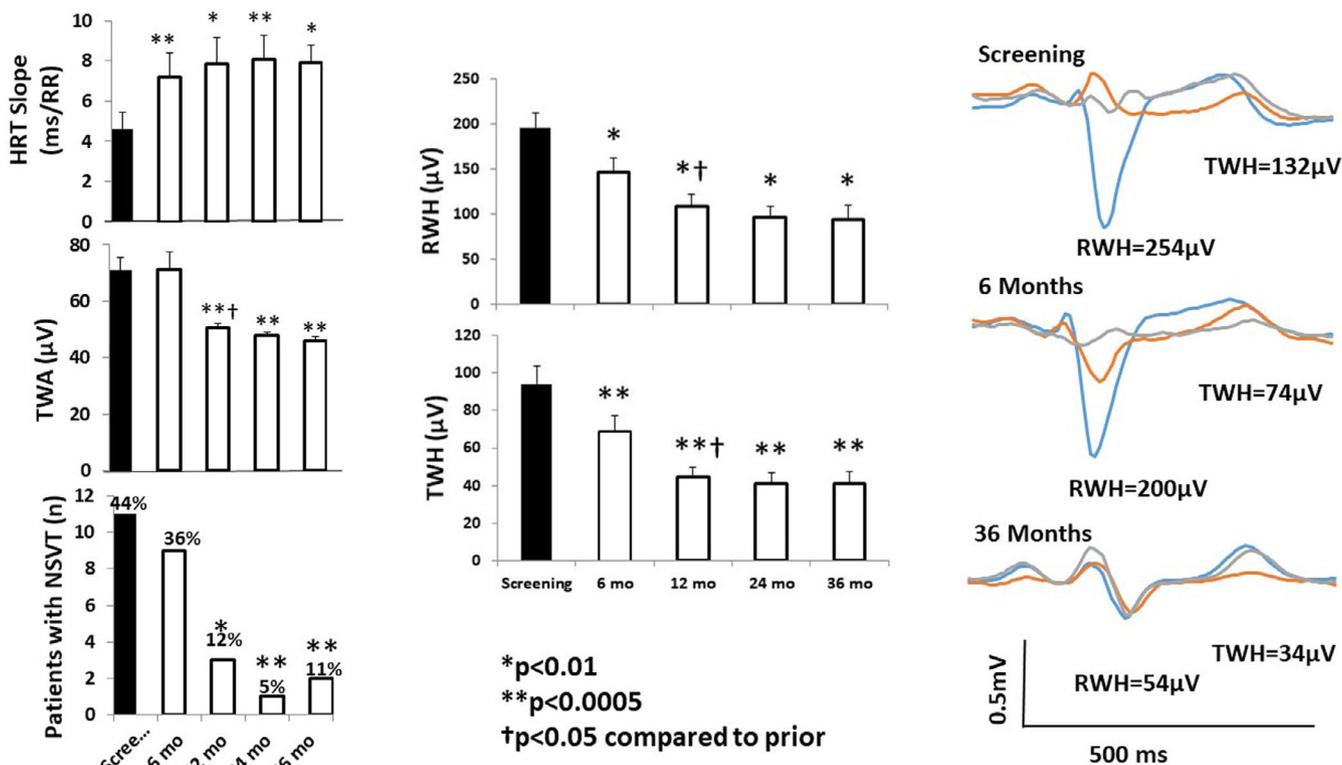

FIGURE 6 Left panel: Time course of effects of vagus nerve stimulation (VNS) therapy on heart rate turbulence (HRT) slope (upper panel), T-wave alternans (TWA) (middle panel), and numbers of patients with nonsustained ventricular tachycardia (NSVT) >3 beats (lower panel) in the Autonomic Neural Regulation Therapy to Enhance Myocardial Function in Heart Failure (ANTHEM-HF) Pilot study. The increase in HRT slope is associated with the beneficial effect of increasing baroreceptor sensitivity. Mean TWA was reduced from >70 μV, a severely abnormal level (≥60 μV), to a normal range (<47 μV). The number of patients with NSVT was also significantly decreased by chronic VNS therapy. Middle panels: Significant improvement in R-wave and T-wave heterogeneity (RWH and TWH) occurred at 6 months following initiation of VNS and persisted throughout the study. Right panel: Substantial, sustained reductions RWH and TWH in a representative study patient. Tracings were obtained at baseline screening and at 6 and 36 months after VNS device implantation. Left panel: *p = .03 compared with screening; **p = .02 compared with screening; †p < .05 compared with prior. Reprinted with permission from Nearing et al. (2021)
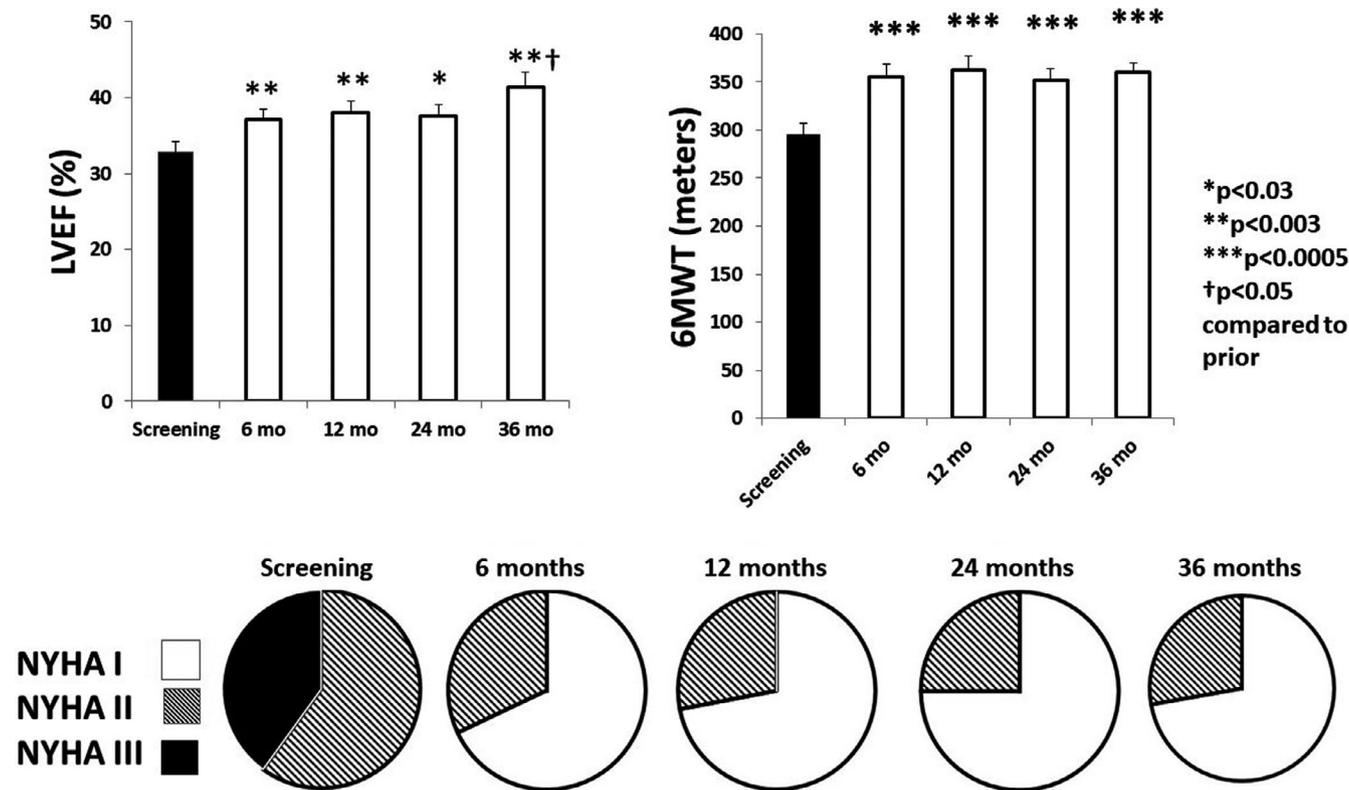
FIGURE 7 Effects of chronic vagus nerve stimulation (VNS) therapy on indices of cardiac performance in the Autonomic Neural Regulation Therapy to Enhance Myocardial Function in Heart Failure (ANTHEM-HF) Pilot study. Significant increases in left ventricular ejection fraction (LVEF) (upper left panel) were documented across the 3-year observation period. A beneficial effect was also observed during the 6-min walk test (6MWT) (upper right panel). All patients exhibited an improvement in New York Heart Association (NYHA) Class status (lower panel). By 6 months, NYHA Class III patients (filled) were all reclassified to NYHA Classes I (open) or II (striped). Reprinted with permission from Nearing et al. (2021)

Olshansky, 2011). Thus, in symptomatic patients with HFrEF, chronic VNS appears to provide wide-ranging, persistent improvements in autonomic tone (HRV), baroreceptor sensitivity (HRT), and cardiac electrical stability (TWA, RWH, and TWH). The Autonomic Neural Regulation Therapy to Enhance Myocardial Function in Heart Failure with Reduced Ejection Fraction (ANTHEM-HFrEF) Pivotal randomized controlled trial (NCT03425422) is currently underway to assess the clinical utility of chronic VNS therapy in comparison with guideline-directed medical therapy (Konstam et al., 2019).

4.7 | ECG heterogeneity for detecting clinically significant coronary artery stenosis

4.7.1 | ETT and pharmacological stress testing

Noninvasive detection of flow-limiting stenoses in large epicardial coronary arteries remains an enduring challenge in contemporary cardiology. Beyond evaluation of symptoms, the main first-line diagnostic techniques for disclosing the presence of coronary artery disease (CAD) are ETT or pharmacologic stress with or without echocardiographic or nuclear myocardial perfusion imaging (MPI). Provocation of ST-segment depression during ETT is the

most widely utilized objective sign of CAD-associated myocardial ischemia. During pharmacologic stress testing, ST-segment evaluation has proved to be unreliable (Rief et al., 2018) and reversible perfusion defects on MPI or inducible echocardiographically apparent wall motion abnormalities are the main indicators of disease.

It is generally recognized that contemporary tests yield excess numbers of both false-positive and false-negative results as compared to diagnostic coronary angiography (Kern et al., 2006). ETT-based detection of coronary artery stenosis using ST-segment measurement is especially problematic in women, and the high false-positive rate ranges from 25% to 50% (Fihn et al., 2014; Stoletniy & Pai, 1997). A number of other ECG parameters in addition to ST-segment deviation have been evaluated to enhance the diagnostic yield of ETT, including ST/heart rate slope or index and ST/heart rate recovery loop (Lachterman et al., 1990; Okin et al., 1989). However, none has been found to provide significant additive diagnostic value in clinical practice.

Characteristics of all 137 patients at our institution who underwent diagnostic coronary angiography within 0 to 5 days after ETT or intravenous dipyridamole infusion in 2016 were studied (Silva et al., 2020). While at rest, TWH levels were similar for cases and controls, ETT and dipyridamole stress testing increased TWH
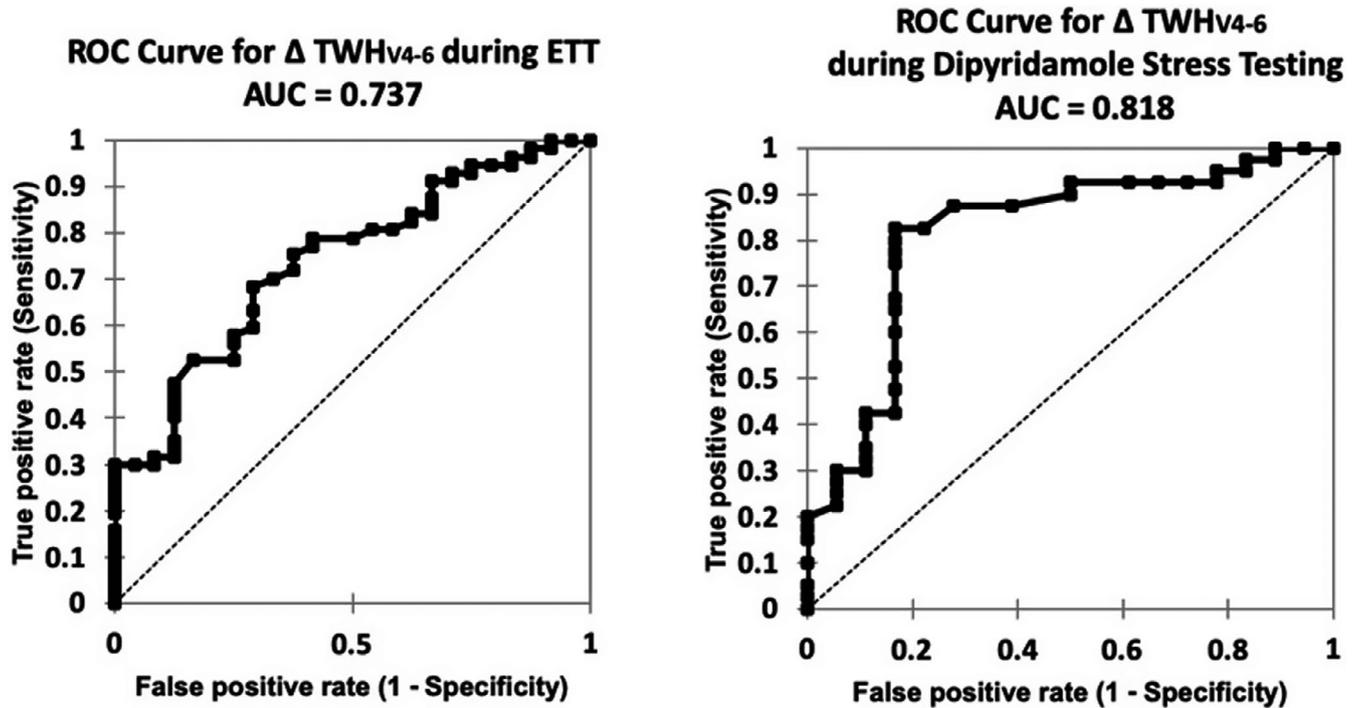
FIGURE 8 Areas under the receiver operating characteristic curve (AUCs) for an increase in T-wave heterogeneity in leads V_{4-6} (TWH$_{V_{4-6}}$) for clinically significant flow-limiting coronary artery stenosis were 0.737 for exercise tolerance testing (ETT) (left panel) and 0.818 for myocardial perfusion imaging (MPI) with dipyridamole (right panel). ST-segment changes with ETT and MPI with dipyridamole did not discriminate cases from controls. Reprinted with permission from Silva et al. (2020)
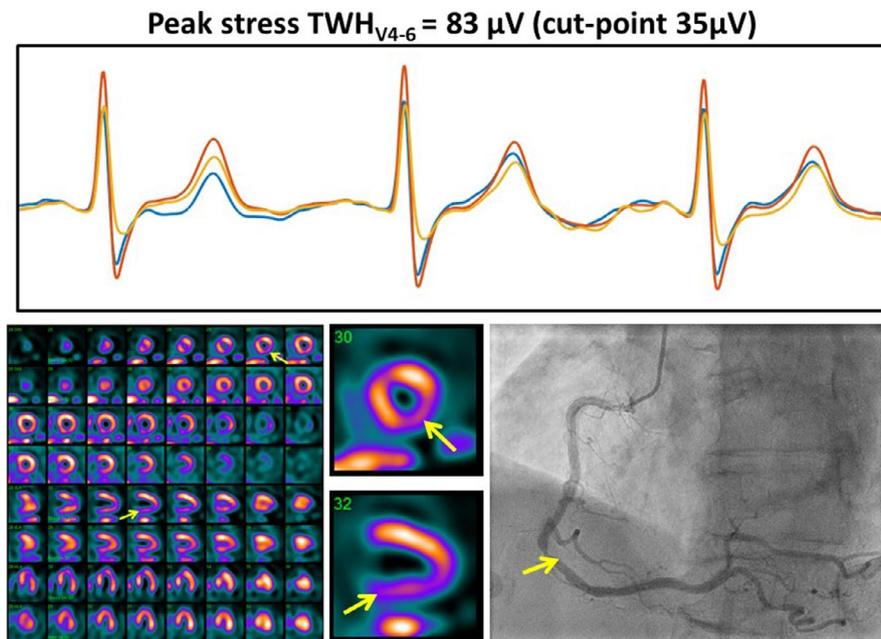

FIGURE 9 True-positive myocardial perfusion imaging (MPI) case confirmed by coronary angiogram showed a sizeable increase in TWH$_{V_{4-6}}$. Regadenoson testing elicited a 30% increase in TWH$_{V_{4-6}}$ to 83 µV in an 81-year-old woman with chest pain (upper panel). Positive MPI revealed a significant lesion in the right coronary artery territory (lower left panel). Coronary angiogram confirmed an 80% lesion in the right coronary artery (lower right panel). The clinical notes indicated reversible, medium-sized, moderate severity perfusion defect involving the LAD territory; transient cavity dilation consistent with multi-vessel or left main disease; and normal left ventricular cavity size and systolic function at rest with stress-induced global hypokinesis. Reprinted with permission from Araujo Silva et al. (2020)

by 69% ($p < .0001$) and 27% ($p < .0001$), respectively, in cases. In controls, TWH did not change. AUCs for TWH increase for any flow-limiting coronary artery stenosis were 0.737 ($p < .0001$) for ETT and 0.818 ($p < .0001$) for dipyridamole stress testing (Figure 8) (Table 1). By contrast, neither ST-segment changes during ETT ($p = .12$) nor MPI during dipyridamole stress testing ($p = .60$) distinguished between cases and controls. These findings support the view that TWH measurement improves detection of angiographically confirmed flow-limiting stenoses in large epicardial coronary arteries during both ETT and MPI during pharmacologic stress testing with dipyridamole.

4.7.2 | Use of regadenoson-induced TWH to complement coronary stenosis detection by myocardial perfusion imaging in men and women

A follow-up study focused on the capacity of TWH_{V4-6} to detect the presence of flow-limiting lesions (FLL) during pharmacologic stress testing with the widely utilized selective A2A adenosine agonist, regadenoson, in conjunction with SPECT MPI (Araujo Silva et al., 2020). The guiding hypotheses were that the heterogeneous coronary blood flow induced by coronary vasodilation imposed by regadenoson in patients with FLL would result in significantly greater nonuniformities of spatiotemporal repolarization in cases than in controls and that these nonuniformities could be assessed by TWH analysis. Accordingly, this investigation tested whether TWH analysis could complement radiographic MPI in identifying FLL confirmed by diagnostic coronary angiography in women and men. Medical records of all 103 patients at our institution who underwent stress testing with regadenoson (0.4 mg IV bolus) within 3 months of coronary angiography from September 2017 to March 2019 were studied. Cases ($n = 59$) had angiographically significant FLL (>50% of left main or >70% of other epicardial coronary arteries ≥2 mm in diameter); controls ($n = 44$) were normal or had non-FLL. Maximum TWH_{V4-6} levels during regadenoson stress were 68% higher in cases than in controls ($p < .0001$). TWH_{V4-6} yielded AUCs of 0.79 in men ($p < .0001$) and 0.71 in women ($p = .007$) (Figure 9) (Table 1). In men, the ROC-guided 54-μV TWH_{V4-6} cutpoint for FLL produced adjusted odds of 7.3 (95% CI: 1.3–41.5, $p = .03$) with 79% sensitivity and 78% specificity. In women, the ROC-guided 35-mV TWH_{V4-6} cutpoint produced adjusted odds of 4.5 (95% CI: 1.1–18.9, $p = .04$) with 84% sensitivity and 52% specificity. Adding TWH_{V4-6} to MPI determinations reduced false-positive results by 70%, more than doubled true-negative results, and improved the adjusted odds ratio to 6.8 (95% CI: 2.2–21.4, $p = .001$) with specificity of 78% in men and 86% in women.

This observational full-cohort study was the first to report that quantitative TWH_{V4-6} can detect the presence of large epicardial coronary artery stenosis during regadenoson pharmacologic stress testing during SPECT MPI. Detection of clinically significant stenoses by TWH_{V4-6} was equivalent in women and men. TWH_{V4-6} and SPECT MPI may have complementary value inasmuch as TWH_{V4-6}

is readily quantifiable and is not disrupted by imaging challenges such as balanced ischemia and tissue attenuation. Imaging provides information regarding the size and location of reversible perfusion defects. Importantly, the improved specificity afforded by combined assessment of TWH_{V4-6} and SPECT MPI provides an approach for decreasing the false-positive rate of stress testing, thereby potentially reducing unnecessary referrals for diagnostic coronary angiography.

5 | LIMITATIONS

Notwithstanding this promising evidence regarding the utility of interlead ECG heterogeneity assessment, a number of significant challenges remain. Among the most notable technical issues are to establish the optimum lead selection for the various conditions in which this method is to be applied. Across the pathologies studied, leads V_4–V_6 appear to be among the most reliable. These leads were originally selected as they exhibit robust T waves with relatively minimum differences in shape among neighboring leads in normal conditions, therefore enabling detection of pathophysiologic changes not affected by baseline differences in resting conditions. Furthermore, based on point-source theory, these leads provide a distinct yet broadly sufficient field of view to detect potential ischemic changes. However, it is possible that other lead configurations, for example, semi-orthogonal lead sets such as I, aVF, and V_3, may improve accuracy in risk assessment.

To date, we have utilized the 10-s beat stream as provided by standard 12-lead ECGs. Whether a smaller number of beats will be sufficient remains to be determined. Noise is always a consideration whenever morphology is assessed, but when skin is well prepared for contact electrodes, the standard ECG filters appear adequate. We have incorporated a template of superimposed beats to facilitate overreading the morphology and ruling out significant noise artifacts.

6 | CONCLUSIONS

A sizeable body of scientific evidence implicates heterogeneity of ECG morphology in the genesis of cardiac arrhythmias, due to the fact that depolarization and repolarization heterogeneity interact to promote ventricular arrhythmogenesis. Several contemporary measures appear promising, particularly those that incorporate measurement of depolarization and repolarization morphology. However, most methods are limited to use in subjects at rest.

In this review, we discussed a relatively novel morphological analysis technique, interlead ECG heterogeneity, which was designed at the outset to be incorporated into diverse clinical platforms including ambulatory ECG and ETT monitoring as well as pharmacologic stress testing. The basic rationale is that the prognostic value could be enhanced by going beyond the snapshot approach and including provocative testing to disclose latent risk for SCD that may not be evident in the resting state. Based on the

performance data including odds ratios and ROCs, it appears that interlead ECG heterogeneity is a promising parameter that stratifies risk for SCD, cardiac death, and arrhythmias under diverse pathophysiologic states including latent cardiac electrical instability, heart failure, and clinically significant coronary stenosis. Extensive multicenter studies will be needed to determine the precise clinical applications for second central moment analysis of R- and T-wave morphology as well as other contemporary measures.

CONFLICT OF INTEREST

The authors declare no conflicts of interest in connection with this article. No funds were received for the preparation of this review.

ETHICAL APPROVAL

The cited studies at Beth Israel Deaconess Medical Center (Boston MA, USA) conformed to the ethical guidelines of the 1975 Declaration of Helsinki and were performed under a protocol approved by the internal review board.

AUTHOR CONTRIBUTIONS

All of the authors contributed to this review by drafting the manuscript and critically reviewing it.

DATA AVAILABILITY STATEMENT

Data sharing is not applicable to this article as no new data were created or analyzed in this study.

ORCID

Richard L. Verrier https://orcid.org/0000-0001-5602-6793

REFERENCES

Antzelevitch, C. (2007). Heterogeneity and cardiac arrhythmias: An overview. *Heart Rhythm*, 4(7), 964–972. https://doi.org/10.1016/j.hrthm.2007.03.036

Araujo Silva, B., Hauser, T. H., Nearing, B. D., Bortolotto, A. L., Marum, A. A., Tessarolo Silva, F., Medeiros, S. A., Pedreira, G. C., Gervino, E. V., & Verrier, R. L. (2020). Regadenoson-induced T-wave heterogeneity complements coronary stenosis detection by myocardial perfusion imaging in men and women. *European Heart Journal - Cardiovascular Imaging*, jeaa128. https://doi.org/10.1093/ehjci/jeaa128

Bonatti, R., Silva, A. F. G., Batatinha, J. A. P., Sobrado, L. F., Machado, A. D., Varone, B. B., Nearing, B. D., Belardinelli, L., & Verrier, R. L. (2014). Selective late sodium current blockade with GS-458967 markedly reduces ischemia-induced atrial and ventricular repolarization alternans and ECG heterogeneity. *Heart Rhythm*, 11(10), 1827–1835. https://doi.org/10.1016/j.hrthm.2014.06.017

Bortolotto, A. L., Verrier, R. L., Nearing, B. D., Marum, A. A., Araujo Silva, B., Pedreira, G. C., Tessarolo Silva, F., Medeiros, S. A., Sroubek, J., Zimetbaum, P. J., & Chang, J. D. (2020). Pre-implantation interlead ECG heterogeneity is superior to QRS complex duration in predicting mechanical super-response in patients with non-left bundle branch block receiving cardiac resynchronization therapy. *Heart Rhythm*, 17(11), 1887–1896. https://doi.org/10.1016/j.hrthm.2020.05.036

Burke, G. M., Araujo Silva, B., Marum, A. A., Bortolotto, A. L., Nearing, B. D., Chen, M .J., Fostello, S., Popma, J. J., Verrier, R. L., & Chang, J. D. (2021). Speckle tracking strain and ECG heterogeneity correlate in transcatheter aortic valve replacement-Induced left bundle branch blocks and right ventricular paced rhythms. *Open Heart*, in press.

Chauhan, V. S., Downar, E., Nanthakumar, K., Parker, J. D., Ross, H. J., Chan, W., & Picton, P. (2006). Increased ventricular repolarization heterogeneity in patients with ventricular arrhythmia vulnerability and cardiomyopathy: A human in vivo study. *American Journal of Physiology. Heart and Circulatory Physiology*, 290(1), H79–86. https://doi.org/10.1152/ajpheart.00648.2005.

Dupont, M., Rickard, J., Baranowski, B., Varma, N., Dresing, T., Gabi, A., Finucan, M., Mullens, W., Wilkoff, B. L., & Tang, W. H. W. (2012). Differential response to cardiac resynchronization therapy and clinical outcomes according to QRS morphology and QRS duration. *Journal of the American College of Cardiology*, 60(7), 592–598. https://doi.org/10.1016/j.jacc.2012.03.059

Fihn, S. D., Blankenship, J. C., Alexander, K. P., Bittl, J. A., Byrne, J. G., Fletcher, B. J., Fonarow, G. C., Lange, R. A., Levine, G. N., Maddox, T. M., Naidu, S. S., Ohman, E. M., & Smith, P. K. (2014). 2014 ACC/AHA/AATS/PCNA/SCAI/STS focused update of the guideline for the diagnosis and management of patients with stable ischemic heart disease. *Journal of the American College of Cardiology*, 64(18), 1929–1949. https://doi.org/10.1016/j.jacc.2014.07.017

Fuller, H., Justo, F., Nearing, B. D., Kahlig, K., Rajamani, S., Belardinelli, L., & Verrier, R. L. (2016). Eleclazine, a new selective cardiac late sodium current inhibitor, confers concurrent protection against autonomically induced atrial premature beats, repolarization alternans and heterogeneity, and atrial fibrillation in an intact porcine model. *Heart Rhythm*, 13, 1679–1686. https://doi.org/10.1016/j.hrthm.2016.04.015

Fuller, M. S., Sándor, György, Punske, B., Taccardi, B., MacLeod, R. S., Ershler, P. R., Green, L. S., & Lux, R. L. (2000). Estimates of repolarization dispersion from electrocardiographic measurements. *Circulation*, 102(6), 685–691. https://doi.org/10.1161/01.CIR.102.6.685

Han, J., & Moe, G. K. (1964). Nonuniform recovery of excitability in ventricular muscle. *Circulation Research*, 14, 44–60. https://doi.org/10.1161/01.res.14.1.44

Higham, P. D., & Campbell, R. W. (1994). QT dispersion. *British Heart Journal*, 71(6), 508–510. https://doi.org/10.1136/hrt.71.6.508

Justo, F., Fuller, H., Nearing, B. D., Rajamani, S., Belardinelli, L., & Verrier, R. L. (2016). Inhibition of the cardiac late sodium current with eleclazine protects against ischemia-induced vulnerability to atrial fibrillation and reduces atrial and ventricular repolarization abnormalities in the absence and presence of concurrent adrenergic stimulation. *Heart Rhythm*, 13, 1860–1867. https://doi.org/10.1016/j.hrthm.2016.06.020

Kenttä, T. V., Nearing, B. D., Porthan, K., Tikkanen, J. T., Viitasalo, M., Nieminen, M. S., Salomaa, V., Oikarinen, L., Huikuri, H. V., & Verrier, R. L. (2016). Prediction of sudden cardiac death with automated high throughput analysis of heterogeneity in standard resting 12-lead electrocardiogram. *Heart Rhythm*, 13, 713–720. https://doi.org/10.1016/j.hrthm.2015.11.035

Kern, M. J., Lerman, A., Bech, J.-W., De Bruyne, B., Eeckhout, E., Fearon, W. F., Higano, S. T., Lim, M. J., Meuwissen, M., Piek, J. J., Pijls, N. H. J., Siebes, M., Spaan, J. A. E., & American Heart Association Committee on Diagnostic and Interventional Cardiac Catheterization, Council on Clinical Cardiology. (2006). Physiological assessment of coronary artery disease in the cardiac catheterization laboratory: A scientific statement from the American Heart Association Committee on Diagnostic and Interventional Cardiac Catheterization. *Circulation*, 114(12), 1321–1341. https://doi.org/10.1161/CIRCULATIONAHA.106.177276

Kolman, B. S., Verrier, R. L., & Lown, B. (1975). The effect of vagus nerve stimulation upon vulnerability of the canine ventricle: Role of sympathetic-parasympathetic interactions. *Circulation*, 52(4), 578–585. https://doi.org/10.1161/01.cir.52.4.578

Konstam, M. A., Udelson, J. E., Butler, J., Klein, H. U., Parker, J. D., Teerlink, J. R., Wedge, P. M., Saville, B. R., Ardell, J. L., Libbus, I., & DiCarlo, L. A. (2019). Impact of autonomic regulation therapy in

patients with heart failure: ANTHEM-HFrEF pivotal study design. *Circulation: Heart Failure*, *12*(11), e005879. https://doi.org/10.1161/CIRCHEARTFAILURE.119.005879

Lachterman, B., Lehmann, K. G., Detrano, R., Neutel, J., & Froelicher, V. F. (1990). Comparison of ST segment/heart rate index to standard ST criteria for analysis of exercise electrocardiogram. *Circulation*, *82*(1), 44–50. https://doi.org/10.1161/01.cir.82.1.44

Levy, M. N., & Blattberg, B. (1976). Effect of vagal stimulation on the overflow of norepinephrine into the coronary sinus during cardiac sympathetic nerve stimulation in the dog. *Circulation Research*, *38*(2), 81–84. https://doi.org/10.1161/01.res.38.2.81

Li, W., & Olshansky, B. (2011). Inflammatory cytokines and nitric oxide in heart failure and potential modulation by vagus nerve stimulation. *Heart Failure Reviews*, *16*(2), 137–145. https://doi.org/10.1007/s10741-010-9184-4

Libbus, I., Nearing, B. D., Amurthur, B., KenKnight, B. H., & Verrier, R. L. (2016). Autonomic regulation therapy suppresses quantitative T-wave alternans and improves baroreflex sensitivity in heart failure patients enrolled in the ANTHEM-HF study. *Heart Rhythm*, *13*, 721–728. https://doi.org/10.1016/j.hrthm.2015.11.030

Malik, M., Acar, B., Gang, Y., Yap, Y. G., Hnatkova, K., & Camm, A. J. (2000). QT dispersion does not represent electrocardiographic interlead heterogeneity of ventricular repolarization. *Journal of Cardiovascular Electrophysiology*, *11*(8), 835–843. https://doi.org/10.1111/j.1540-8167.2000.tb00061.x

Monteiro, F. R., Rabelo Evangelista, A. B., Nearing, B. D., Medeiros, S. A., Tessarolo Silva, F., Pedreira, G. C., Ullman, E., Gervino, E. V., & Verrier, R. L. (2021). T-wave heterogeneity in standard resting 12-lead ECGs is associated with 90-day cardiac mortality in women following emergency department admission: A nested case–control study. *Annals of Noninvasive Electrocardiology*, *26*(3), e12826. https://doi.org/10.1111/anec.12826

Moss, A. J., Hall, W. J., Cannom, D. S., Klein, H., Brown, M. W., Daubert, J. P., Estes, N. A. M., Foster, E., Greenberg, H., Higgins, S. L., Pfeffer, M. A., Solomon, S. D., Wilber, D., & Zareba, W. (2009). Cardiac-resynchronization therapy for the prevention of heart-failure events. *New England Journal of Medicine*, *361*(14), 1329–1338. https://doi.org/10.1056/NEJMoa0906431

Nearing, B. D., Anand, I. S., Libbus, I., Dicarlo, L. A., Kenknight, B. H., & Verrier, R. L. (2021). Vagus nerve stimulation provides multiyear improvements in autonomic function and cardiac electrical stability in the ANTHEM-HF study. *Journal of Cardiac Failure*, *27*(2), 208–216. https://doi.org/10.1016/j.cardfail.2020.10.003

Nearing, B. D., & Verrier, R. L. (2003). Tracking cardiac electrical instability by computing interlead heterogeneity of T-wave morphology. *Journal of Applied Physiology*, *95*(6), 2265–2272. https://doi.org/10.1152/japplphysiol.00623.2003

Nearing, B. D., & Verrier, R. L. (2015). Multilead template-derived residua of surface ECGS for quantitative assessment of arrhythmia risk. *Annals of Noninvasive Electrocardiology*, *20*(3), 273–281. https://doi.org/10.1111/anec.12205

Nearing, B. D., Wellenius, G. A., Mittleman, M. A., Josephson, M. E., Burger, A. J., & Verrier, R. L. (2012). Crescendo in depolarization and repolarization heterogeneity heralds development of ventricular tachycardia in hospitalized patients with decompensated heart failure. *Circulation: Arrhythmia and Electrophysiology*, *5*(1), 84–90. https://doi.org/10.1161/CIRCEP.111.965434

Okin, P. M., Ameisen, O., & Kligfield, P. (1989). Recovery-phase patterns of ST segment depression in the heart rate domain. Identification of coronary artery disease by the rate-recovery loop. *Circulation*, *80*(3), 533–541. https://doi.org/10.1161/01.cir.80.3.533

Okin, P. M., Xue, Q., Reddy, S., & Kligfield, P. (2000). Electrocardiographic quantitation of heterogeneity of ventricular repolarization. *Annals of Noninvasive Electrocardiology*, *5*, 79–87.

Panikkath, R., Reinier, K., Uy-Evanado, A., Teodorescu, C., Hattenhauer, J., Mariani, R., Gunson, K., Jui, J., & Chugh, S. S. (2011). Prolonged Tpeak-to-tend interval on the resting ECG is associated with increased risk of sudden cardiac death. *Circulation: Arrhythmia and Electrophysiology*, *4*(4), 441–447. https://doi.org/10.1161/CIRCEP.110.960658

Porthan, K., Viitasalo, M., Jula, A., Reunanen, A., Rapola, J., Väänänen, H., Nieminen, M. S., Toivonen, L., Salomaa, V., & Oikarinen, L. (2009). Predictive value of electrocardiographic QT interval and T-wave morphology parameters for all-cause and cardiovascular mortality in a general population sample. *Heart Rhythm*, *6*(8), 1202–1208.e1. https://doi.org/10.1016/j.hrthm.2009.05.006

Porthan, K., Viitasalo, M., Toivonen, L., Havulinna, A. S., Jula, A., Tikkanen, J. T., Väänänen, H., Nieminen, M. S., Huikuri, H. V., Newton-Cheh, C., Salomaa, V., & Oikarinen, L. (2013). Predictive value of electrocardiographic T-wave morphology parameters and T-wave peak to T-wave end interval for sudden cardiac death in the general population. *Circulation: Arrhythmia and Electrophysiology*, *6*(4), 690–696. https://doi.org/10.1161/CIRCEP.113.000356

Prenner, S. B., Shah, S. J., Goldberger, J. J., & Sauer, A. J. (2016). Repolarization heterogeneity: Beyond the QT interval. *Journal of the American Heart Association*, *5*(5), e003607. https://doi.org/10.1161/JAHA.116.003607

Rautaharju, P. M. (2002). Why did QT dispersion die? *Cardiac Electrophysiology Review*, *6*(3), 295–301. https://doi.org/10.1023/a:1016397529393

Rickard, J., Kumbhani, D. J., Popovic, Z., Verhaert, D., Manne, M., Sraow, D., Baranowski, B., Martin, D. O., Lindsay, B. D., Grimm, R. A., Wilkoff, B. L., & Tchou, P. (2010). Characterization of super-response to cardiac resynchronization therapy. *Heart Rhythm*, *7*(7), 885–889. https://doi.org/10.1016/j.hrthm.2010.04.005

Rief, M., Chen, M. Y., Vavere, A. L., Kendziora, B., Miller, J. M., Bandettini, W. P., Cox, C., George, R. T., Lima, J., Di Carli, M., Plotkin, M., Zimmermann, E., Laule, M., Schlattmann, P., Arai, A. E., & Dewey, M. (2018). Coronary artery disease: Analysis of diagnostic performance of CT perfusion and Mr Perfusion imaging in comparison with quantitative coronary angiography and SPECT-multicenter prospective trial. *Radiology*, *286*(2), 461–470. https://doi.org/10.1148/radiol.2017162447

Silva, A. C., de Antonio, V. Z., Sroubek, J., Gervino, E., Ho, K., Medeiros, S. A., Silva, F. T., Pedreira, G. C., Stocco, F. G., Nearing, B. D., & Verrier, R. L. (2020). Exercise and pharmacologic stress-induced interlead T-wave heterogeneity analysis to detect clinically significant coronary artery stenosis. *International Journal of Cardiology*, *298*, 32–38. https://doi.org/10.1016/j.ijcard.2019.07.066

Solomon, S. D., Zelenkofske, S., McMurray, J. J. V., Finn, P. V., Velazquez, E., Ertl, G., Harsanyi, A., Rouleau, J. L., Maggioni, A., Kober, L., White, H., Van de Werf, F., Pieper, K., Califf, R. M., Pfeffer, M. A., & Valsartan in Acute Myocardial Infarction Trial (VALIANT) Investigators. (2005). Sudden death in patients with myocardial infarction and left ventricular dysfunction, heart failure, or both. *New England Journal of Medicine*, *352*(25), 2581–2588. https://doi.org/10.1056/NEJMoa043938

Stoletniy, L. N., & Pai, R. G. (1997). Value of QT dispersion in the interpretation of exercise stress test in women. *Circulation*, *96*(3), 904–910. https://doi.org/10.1161/01.cir.96.3.904

Surawicz, B. (1996). Will QT dispersion play a role in clinical decision-making? *Journal of Cardiovascular Electrophysiology*, *7*(8), 777–784. https://doi.org/10.1111/j.1540-8167.1996.tb00583.x

Tan, A. Y., Nearing, B. D., Rosenberg, M., Nezafat, R., Josephson, M. E., & Verrier, R. L. (2017). Interlead heterogeneity of R- and T-wave morphology in standard 12-lead ECGs predicts sustained ventricular tachycardia/fibrillation and arrhythmic death in patients with cardiomyopathy. *Journal of Cardiovascular Electrophysiology*, *28*, 1324–1333. https://doi.org/10.1111/jce.13288

Tomassoni, G. (2016). How to define cardiac resynchronization therapy response. *Journal of Innovations in Cardiac Rhythm Management*, *7*, S1–S7.

Verrier, R. L., & Huikuri, H. V. (2017). Tracking interlead heterogeneity of R- and T-wave morphology to disclose latent risk for sudden cardiac death. *Heart Rhythm*, *14*, 1466–1475. https://doi.org/10.1016/j.hrthm.2017.06.017

Verrier, R. L., Klingenheben, T., Malik, M., El-Sherif, N., Exner, D. V., Hohnloser, S. H., Ikeda, T., Martínez, J. P., Narayan, S. M., Nieminen, T., & Rosenbaum, D. S. (2011). Microvolt T-wave alternans physiological basis, methods of measurement, and clinical utility–consensus guideline by International Society for Holter and Noninvasive Electrocardiology. *Journal of the American College of Cardiology*, *58*(13), 1309–1324. https://doi.org/10.1016/j.jacc.2011.06.029

Verrier, R. L., Kumar, K., & Nearing, B. D. (2009). Basis for sudden cardiac death prediction by T-wave alternans from an integrative physiology perspective. *Heart Rhythm*, *6*, 416–422. https://doi.org/10.1016/j.hrthm.2008.11.019

Verrier, R. L., Pagotto, V. P., Kanas, A. F., Sobrado, M. F., Nearing, B. D., Zeng, D., & Belardinelli, L. (2013). Low doses of ranolazine and dronedarone in combination exert potent protection against atrial fibrillation and vulnerability to ventricular arrhythmias during acute myocardial ischemia. *Heart Rhythm*, *10*(1), 121–127. https://doi.org/10.1016/j.hrthm.2012.09.015

Virani, S. S., Alonso, A., Benjamin, E. J., Bittencourt, M. S., Callaway, C. W., Carson, A. P., Chamberlain, A. M., Chang, A. R., Cheng, S., Delling, F. N., Djousse, L., Elkind, M. S. V., Ferguson, J. F., Fornage, M., Khan, S. S., Kissela, B. M., Knutson, K. L., Kwan, T. W., Lackland, D. T., … Tsao, C. W. (2020). Heart disease and stroke statistics-2020 update: A report from the American Heart Association. *Circulation*, *141*(9), e139–e596. https://doi.org/10.1161/CIR.0000000000000757

Waks, J. W., Sitlani, C. M., Soliman, E. Z., Kabir, M., Ghafoori, E., Biggs, M. L., Henrikson, C. A., Sotoodehnia, N., Biering-Sørensen, T., Agarwal, S. K., Siscovick, D. S., Post, W. S., Solomon, S. D., Buxton, A. E., Josephson, M. E., & Tereshchenko, L. G. (2016). Global electric heterogeneity risk score for prediction of sudden cardiac death in the general population: The atherosclerosis risk in communities (ARIC) and cardiovascular health (CHS) studies. *Circulation*, *133*(23), 2222–2234. https://doi.org/10.1161/CIRCULATIONAHA.116.021306

Weiss, J. N., Qu, Z., Chen, P.-S., Lin, S.-F., Karagueuzian, H. S., Hayashi, H., Garfinkel, A., & Karma, A. (2005). The dynamics of cardiac fibrillation. *Circulation*, *112*(8), 1232–1240. https://doi.org/10.1161/CIRCULATIONAHA.104.529545

Wit, A. L., & Janse, M. J. (1992). Experimental models of ventricular tachycardia and fibrillation caused by ischemia and infarction. *Circulation*, *85*(1 Suppl), I32–I42.

Zabel, M., Acar, B., Klingenheben, T., Franz, M. R., Hohnloser, S. H., & Malik, M. (2000). Analysis of 12-lead T-wave morphology for risk stratification after myocardial infarction. *Circulation*, *102*(11), 1252–1257. https://doi.org/10.1161/01.cir.102.11.1252

Zhao, S. X., Lee, L. M., Nearing, B. D., Busso, V. O., Kwaku, K. F., & Verrier, R. L. (2006). Suppression of calcium-induced repolarization heterogeneity as a mechanism of nitroglycerin's antiarrhythmic action. *Journal of Cardiovascular Pharmacology*, *48*(2), 22–29. https://doi.org/10.1097/01.fjc.0000244677.49969.73